Engineering Geology 306 (2022) 106729

Contents lists available at ScienceDirect

Engineering Geology

journal homepage: www.elsevier.com/locate/enggeo

Assessment of Distributed Acoustic Sensing (DAS) performance for geotechnical applications

Matteo Rossi [a,*], Roger Wisén [b], Giulio Vignoli [c,d,**], Mauro Coni [c]

[a] Lund University, Lund, Sweden
[b] Impakt Geofysik AB, Sweden
[c] University of Cagliari, Cagliari, Italy
[d] Geological Survey of Denmark and Greenland, Aarhus, Denmark

ARTICLE INFO

Keywords:
Distributed Acoustic Sensing
Surface waves
Geophysical characterization
Artificial stabilization

ABSTRACT

Distributed Acoustic Sensing (DAS) is a recent technology that acquires acoustic vibrations via fiber optics sensors. The utilization of such technique for near-surface geotechnical applications has great potential, especially for the characterization and verification of artificially stabilized ground.

A popular procedure to stabilize the superficial ground (for example, for the preparation of infrastructure subgrade) is the blend of the natural shallower layer with a binder (lime and/or cement). Quality control is required when the binder hardens, and acoustic surveys are an option for non-invasive and non-destructive testing. Relevant parameters to validate the effectiveness of the stabilization procedure are the mechanical properties of the materials. The distribution of shear-wave velocities in the ground is a critical parameter for the geotechnical characterization, since it depends directly on the shear-modulus of the media.

The present experiment verifies the applicability of DAS technology in such geotechnical contexts, which can be representative of a wide range of utilizations, spanning, for example, from road and pavement design to building constructions. The discussed test focuses on the spectral content of the acquired signal and on the estimation of the shear-wave distribution, and compares the DAS responses against signals measured during more traditional seismic surveys using standard geophones.

Despite the inevitable differences between the datasets collected with the different techniques, all the reconstructed shear-wave velocity profiles effectively identify the stabilized soil layer. Also for this reason, one of the main conclusions is that, for geotechnical characterizations, DAS can be a convenient non-invasive alternative to more standard approaches.

1. Introduction

Distributed Acoustic Sensing (DAS) is a recent development (last decade) of fiber optic technologies. DAS records acoustic waves, measuring the variations of Rayleigh backscattering of a laser pulse due to an axial strain of the fiber subjected to elastic vibrations (Fernández-Ruiz et al., 2020; Soga and Luo, 2018).

The methodology showed high potential in different applications. The most common application is probably for deep seismic explorations through Vertical Seismic Profiling (VSP) (Binder et al., 2020; Luo et al., 2021a; Titov et al., 2021; Wilson et al., 2021; Wu et al., 2017).

Seismic passive monitoring at the ground surface is a DAS application with an increasing range of usages in terms of operational conditions and scales. For example, DAS is applied in glaciated terrains to record microseismicity (Walter et al., 2020), as well as for seismological surveys when exploiting the measurements from underwater "dark fibers", even if fiber optics exhibit higher sensitivity to S-waves than P-waves (Cheng et al., 2021; Lior et al., 2021). Other applications include the passive monitoring of volcanic earthquakes to infer the subsurface geological structures (Nishimura et al., 2021). In addition, passive acoustic acquisitions by means of fiber optics are effectively utilized for near-surface characterization of shear-wave velocity distributions (Dou et al., 2017; Luo et al., 2021b; Yuan et al., 2020).

An issue while using DAS for seismological surveys lies in the

* Corresponding author.
** Corresponding author.
E-mail addresses: matteo.rossi@tg.lth.se (M. Rossi), gvignoli@unica.it (G. Vignoli).

https://doi.org/10.1016/j.enggeo.2022.106729
Received 15 October 2021; Received in revised form 4 May 2022; Accepted 22 May 2022
Available online 27 May 2022

impossibility to retrieve the absolute ground displacement as inertial seismometers. The transfer function between ground vibration and fiber optic strain needs to be calibrated, as presented, e.g., by Lindsey et al. (2020). On the contrary, common applied geophysical surveys do not require the knowledge of the absolute ground displacement. This characteristic is in common with traditional geophones used for engineering geology characterizations, which record relative ground vibrations as voltage amplitudes.

The present work focuses on a pilot test in the context of a near-surface geophysical survey for a civil engineering application. We explore the possibility of using DAS for assessing ground elastic parameters in a construction site and we compare the results against traditional geophones receivers to assess the capabilities and the limitations of the DAS technology. The investigated construction site is characterized by an artificially stabilized ground.

Ground stabilization is an engineering application (Firoozi et al., 2017) that faces an increasing demand for exploiting areas with poor bearing capacity. Generally, it results in large financial savings compared to alternative methods. In many cases, ground stabilization is the only practical and economically viable possibility. Ground stabilization is very attractive also from a sustainability perspective regarding natural resources: firstly, it is possible to utilize local material that would otherwise become a landfill problem, and, secondly, it saves valuable raw materials in the form of natural gravel or crushed rock. Utilizing local materials also reduces the need for transport, thus, in turn, it contributes to decrease carbon dioxide emissions. In the case of surface stabilization, a binder is milled into a layer of ground material (usually the shallower decimeters). Once the binder is hardened, quality control is required and, in this respect, seismic measurements can be used as non-invasive and non-destructive testing (Donohue and Long, 2008; Lin et al., 2017).

Clearly, the applicability of the proposed methodology can be extended to monitor, for example, the long-term performances of roads and pavements (Wang et al., 2013). In these cases, the durability assessment should not be limited to what can be inferred from the surface – e.g., by means of the falling weight deflectometer (Coni et al., 2018; Coni et al., 2021) or core drilling (Miskiewicz et al., 2018) – but it should also include information deduced from inside the structure and via sensors located at exactly the same positions during the long-time monitoring (Kara De Maeijer et al., 2019).

2. Methodology

In the present research, the geophysical survey has been performed on top of a slab of stabilized ground, on an active construction site. We acquired acoustic data simultaneously by employing fiber optics and geophones as seismic receivers. The data acquisition has been extended outside the ground-stabilized area with the aim of having also reference measurements on the natural ground.

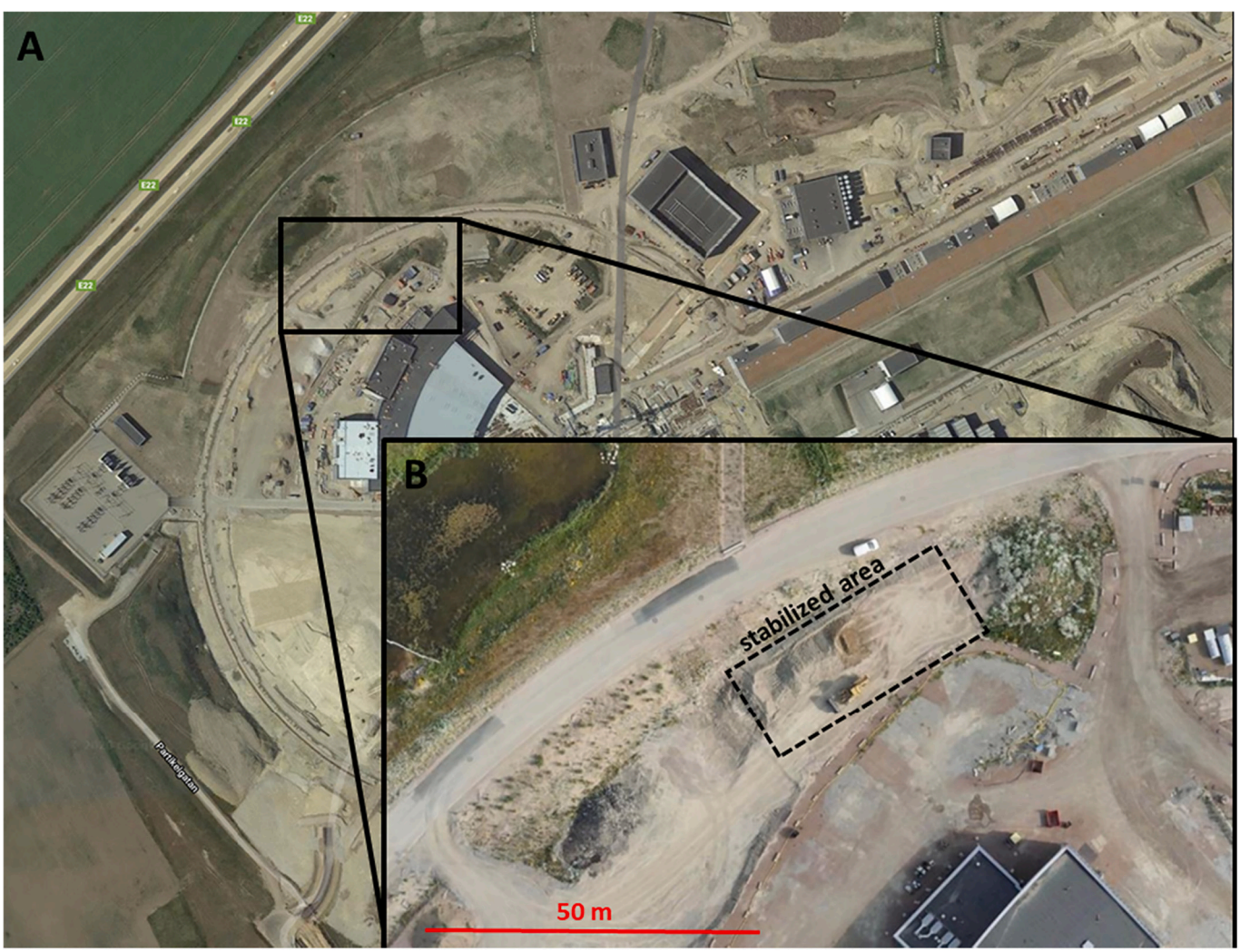

Fig. 1. A) Google Map aerial image (Imagery ©2019, Google) of the construction site. B) Orthophoto of the area during the construction of the stabilized slab (courtesy of Skanska ESS Construction AB).

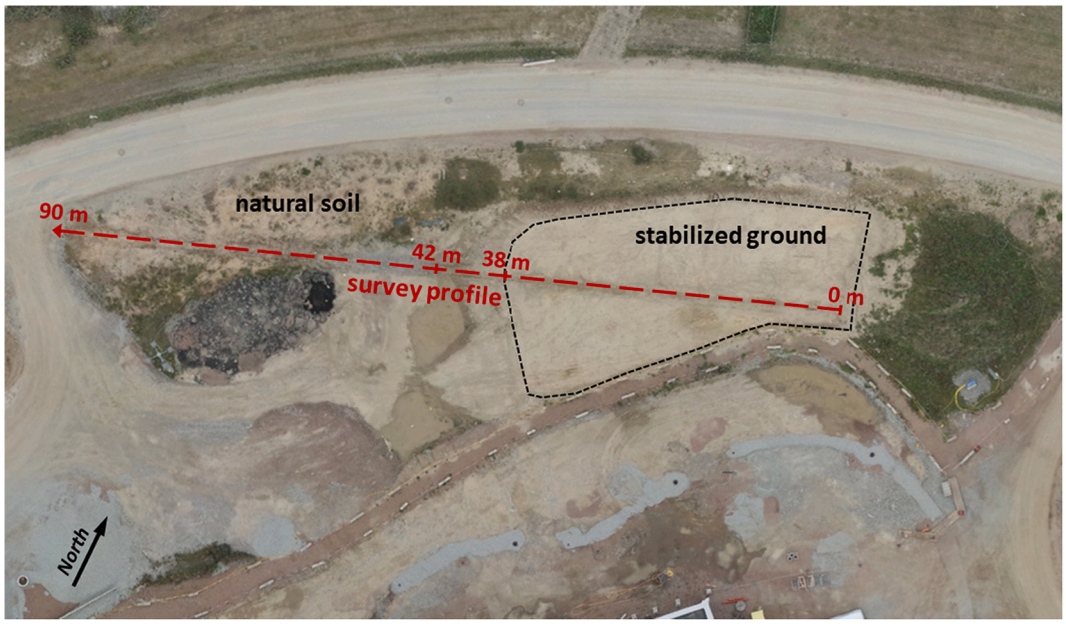

Fig. 2. Location of the survey profile with the local coordinates used for the different acquired layouts. The orthophoto (courtesy of Skanska ESS Construction) has been acquired shortly after the geophysical survey; the mark of the trench on the topsoil is still partially visible.

Fig. 3. Pictures of the installation of the fiber optic cable in the ground: left, digging of the trench; middle, cable on top of sand layer; right, backfilling of the ditch with sand and excavated material.

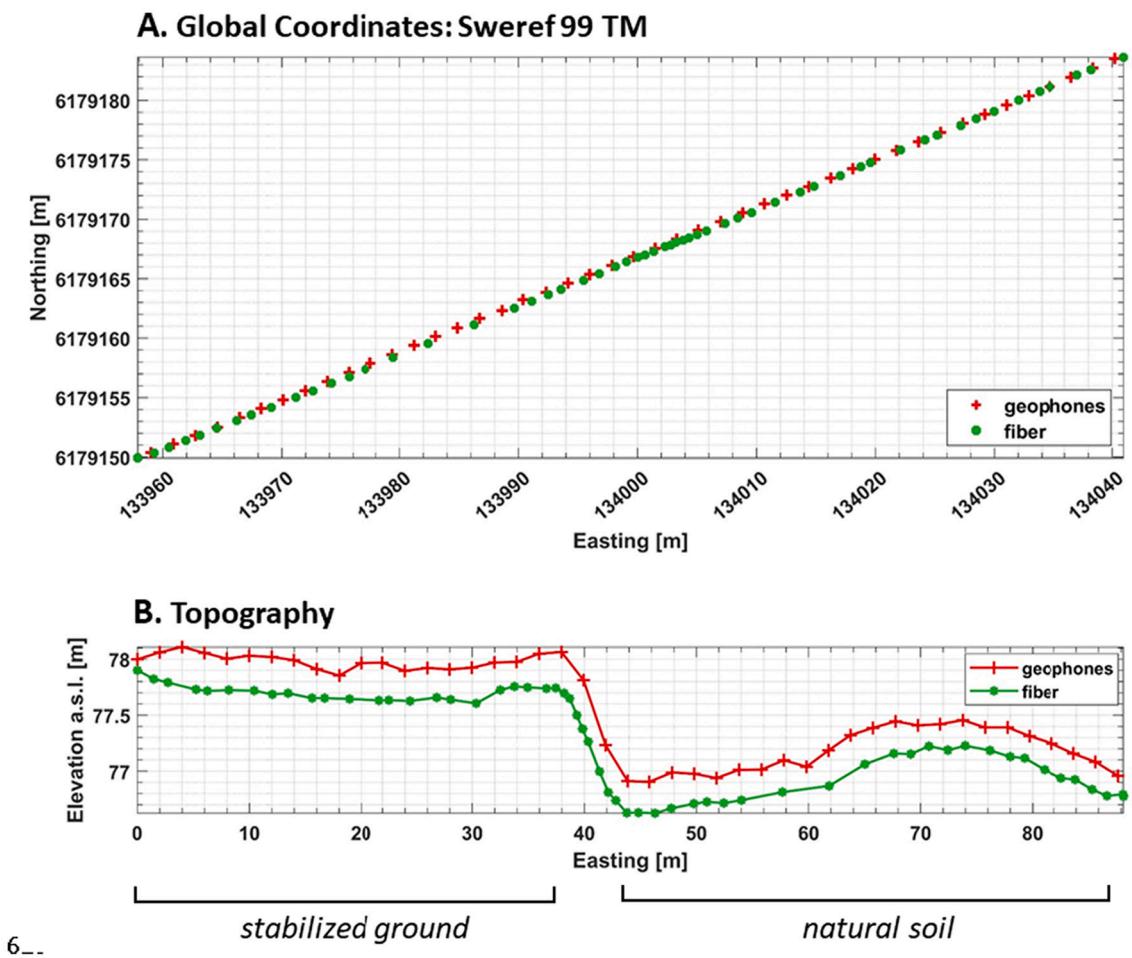

Fig. 4. Global coordinates of the location of the fiber optic cable (green) and the geophones (red). Plot A shows the planar Sweref 99 TM coordinates, whereas panel B shows the elevation above sea level of the sensors along the profile. (For interpretation of the references to colour in this figure legend, the reader is referred to the web version of this article.)

Table 1
Acquisition parameters for the different acoustic systems used at the ESS test. For the local coordinates of the profile, see Fig. 2.

	Fiber optic	Layout 1	Layout 2	Layout 3
	(Carina)	(geophones)	(geophones)	(geophones)
Spatial resolution [m]	2	punctual	punctual	punctual
Spatial sampling [m]	0.255	2	2	0.5
Time sampling interval [s]	$2e^{-5}$	$1.25e^{-4}$	$1.25e^{-4}$	$1.25e^{-4}$
Time window [s]	1.2	1.2	1.2	1.2
Local coordinates along the profile [m]	0–89	0–88	1–89	5–29

2.1. Experimental site

A construction site has been selected for conducting seismic surveys both via DAS and traditional geophones acquisitions. The experimental site is in the municipality of Lund (Sweden), where the European Spallation Source (ESS) facility was under construction (Fig. 1). We focused the experimental test on an area where a slab of stabilized quaternary deposit was constructed through the mixing of natural material and lime cement. The stabilization procedure consists of alternating layers of natural material – excavated from adjacent areas – and lime cement. The improved mechanical properties are supposed to be obtained through mechanical compaction and artificially increased moisture content, necessary for facilitating the chemical reactions of the binder.

The natural material consists of a clayey-silty till deposit on top of a metamorphic crystalline bedrock. The Quaternary sediment is structured in layers with variable granulometric size distributions, where sand or silt-clay could be predominant. The depth to bedrock is around 10 m from the topographic surface and presents a top layer of weathered rock with a thickness of about 1.5 m. The geological information is collected from geotechnical drilling placed about 100 m south of the site and the topographic elevation at the drilling location is about 1 m higher than the investigated area.

The stabilized material covers an area of approximately 30 m by 20 m (Fig. 1) and is characterized by a thickness of about 1–1.5 m. The stabilized slab is covered by an artificial layer of about 0.5 m composed of nearby natural glacial sediments.

A geophysical profile of 90 m has been designed with the aim of investigating both the stabilized and the natural ground (Fig. 2). Along the profile, a 30 cm deep trench has been excavated to install the fiber optic cable within the ground (Fig. 3). This procedure is essential to ensure a good coupling between the cable and the surrounding material and is crucial for the transmission of acoustic energy from the ground to the cable. The fiber optic cable was placed in the ditch on a 2–3 cm bed of medium grain sand to avoid damage to the fiber. Damages might happen during the filling operation if the cable is in contact with large cobbles that might be present in the glacial material. The trench has

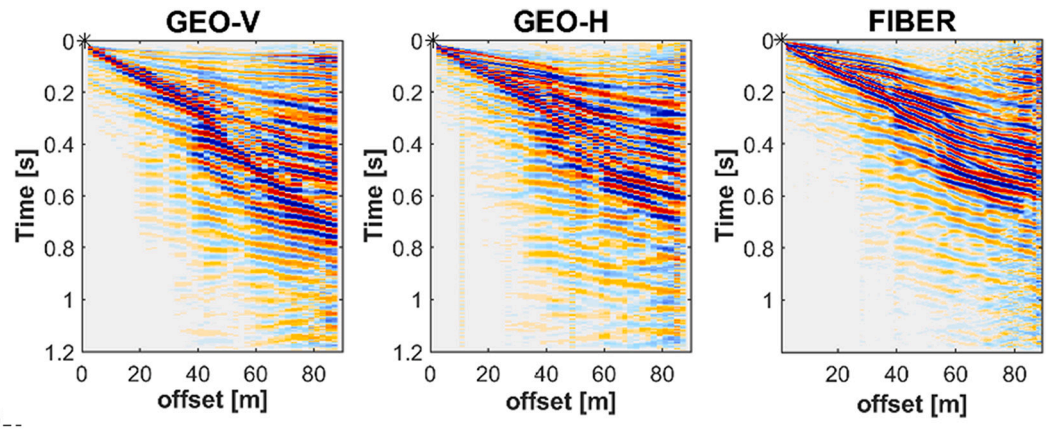

Fig. 5. Example of trace-normalized seismograms from Layout 1 survey: left, vertical geophones (GEO-V); middle, horizontal in-line geophones (GEO-H); right, fiber optic sensors (FIBER). The black asterisk is the location of the source.

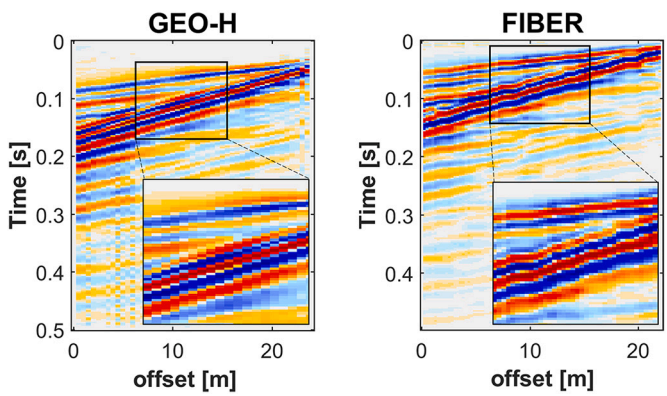

Fig. 6. Example of trace-normalized seismograms from Layout 3: left, horizontal in-line geophones (GEO-H); right, fiber optic sensors (FIBER). It is visible the effect of the 2 m resolution in the fiber optic data.

been backfilled with an analogous thin layer of sand and the material previously excavated. The backfilled ditch has been compacted by the wheels of a heavy machine.

The geophones were placed on top of the installed fiber optic cable and they resulted to be precisely collocated as it is clear from the differential GNSS coordinates acquired along the fiber optic cable and at the geophone locations (Fig. 4A). By checking the elevation of the sensors (Fig. 4B), the position of the cable in the ground is about 0.30 m from the surface, across the entire profile. In addition, the higher elevation of the artificial ground compared to the natural condition is evident.

2.2. DAS system

DAS is a technology that enables real-time measurements of strain and acoustic vibrations along the entire length of a fiber optic cable. The instrument utilized in the experiment is the Carina Sensing System technology (Silixa ltd), which includes an iDAS v3 interrogator and an engineered ("constellation") fiber.

The iDAS is a time domain, single-pulse, phase-based DAS instrument. It works by emitting a pulse of laser light into the optical fiber. As the pulse of light travels down the optical path, interacts within the fiber material resulting in backscattered light reflections. Variations in the amount of backscattered energy are determined by strain events within the fiber, which, in turn, are caused by localized acoustic energy (Lindsey et al., 2020). The time synchronization of the laser pulse allows the backscatter event to be accurately mapped to a fiber distance. The result is the continuous acoustic sampling along the entire length of the optical fiber with a frequency range from a few mHz to over 100 kHz.

The particular type of fiber ("constellation") applied in the present work is developed by Silixa ltd in the attempt to increase the Signal to Noise Ratio (SNR). Engineered bright scatters are implemented along the fiber to enhance the amount of reflected light without introducing significant excess loss in the forward propagating scattered light.

The Carina Sensing System technology was selected for the experiment since the near-surface engineering application needed high spatial resolution to resolve the shallower layers of the ground, which is the main goal of the survey. The other possibly available technical solutions would have not provided the same SNR at such a short spatial resolution.

2.3. Traditional geophone-receivers' system

The traditional geophone-receivers' system consists of a Summit X One seismograph (DMT Group) with a maximum number of 98 4.5 Hz-geophones. Half of the receivers measure the vertical component (GEO-*V*), whereas the remaining sensors record the horizontal component aligned with the profile direction (GEO-H). The vertical and horizontal geophones are located as close as possible in order to obtain 2-component soundings.

2.4. Survey

The survey was performed on the 4th of September 2019. The source of active acoustic waves consisted of an accelerated weight drop (ESS100 Turbo) applied vertically on a metallic plate. This kind of source was necessary to transmit enough energy into the ground and limit the detrimental effects of environmental noise. Coherent noise sources mainly consisted of nearby active construction activities and of heavy vehicular traffic along Highway E22 (visible in the northwest corner of Fig. 1).

Along the investigated profile, we acquired three datasets by using three geophone layouts; each of them characterized by different locations and spacing intervals of the receivers. Contextually, the performed DAS acquisition always involved the entire profile with fixed spatial parameters. Table 1 summarizes the parameters of the acquisition for both acoustic techniques (geophones and DAS).

Layout 1 and Layout 2 are characterized by 2 m inter-geophone spacing for a total length of 88 m (45 2-component receiver stations were deployed); this length was enough to cover both the portion of stabilized ground and the area of natural ground (Fig. 2). Layout 2 is analogue to Layout 1; the only difference is that Layout 2 is shifted by 1 m forward, along the profile. This provides the possibility to combine the two layouts and eventually obtain a profile with a 1 m resolution.

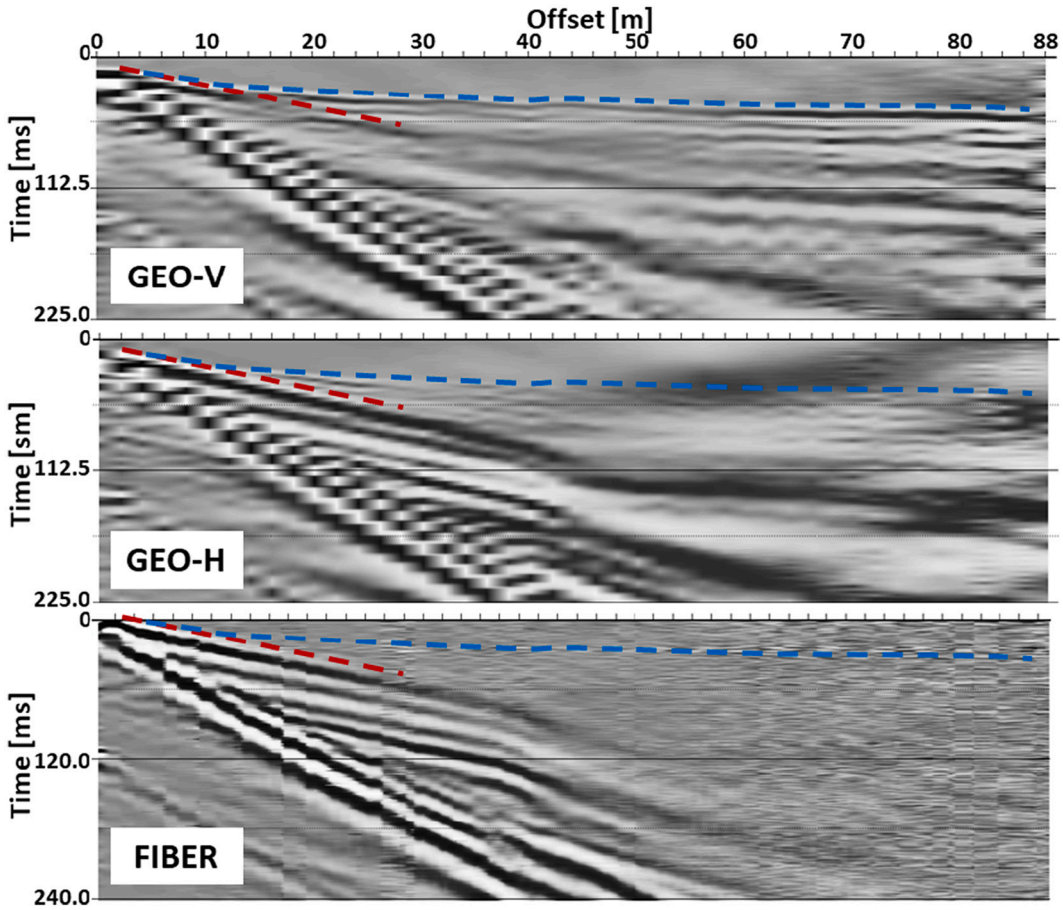

Fig. 7. Seismograms from Layout 1 (2 m geophone spacing) of (from top to bottom): vertical geophones (GEO-V), horizontal in-line geophones (GEO-H) and fiber optic sensors (FIBER). Direct wave and first arrival are picked from GEO-V seismogram and highlighted by red and blue dashed lines, respectively. The two events from GEO-V are superimposed on the other seismograms. (For interpretation of the references to colour in this figure legend, the reader is referred to the web version of this article.)

The integration of Layout 1 and 2 has been done via stacking the seismograms with the same source location, after careful processing and adjustments of zero time. For comparison, also the fiber optic data have been stacked.

Layout 3 has a geophone spacing of 0.5 m for a profile length of 24 m (49 two-component receiver stations) and it is entirely located on the slab of stabilized material.

The DAS surveys are characterized by a characteristic Gauge length, which is the length of the fiber used to calculate the difference in the phase of the backscattered light. The recorded signal is thus averaged along a stretch of the fiber that is centered around the receiver position (Hartog, 2017). The spatial resolution is directly proportional to the Gauge length (Titov et al., 2021; Alfataierge et al., 2020) and, in the specific case under investigation, it equals 2 m.

2.5. Data processing and inversion

Following a quite standard procedure for the extraction of the dispersion curve from the seismic data recorded either with the geophone or with the fiber optics sensors (e.g.: Lai et al., 2002; Socco et al., 2010), the dependence of the Rayleigh wave velocities on the frequency can be deduced via a 2D Fourier transform of the collected seismograms. The result of the Fourier mapping between the time-distance space into the frequency-wavenumber space is usually called FK spectrum. The approach based on these integral transformations ensures the retrieval of more robust information; however, in the attempt of capturing the lateral velocity variations, alternative approaches have been recently developed (e.g.: Vignoli et al., 2011; Bergamo et al., 2012; Vignoli et al., 2016). In our specific test, as we assumed no significant lateral changes along the acquisition lines, after splitting the profile in stabilized and natural ground (Fig. 2), we made full use of the most common technique. Hence, the dispersion curves have been extracted via a simple picking, frequency-by-frequency, of the maxima of the FK spectrum. Dispersion curves describe the dependence of the surface wave (group and/or phase) velocities on the frequencies (and, in turn, on the investigated depth); so, they can be inverted by using 1-D forward modelling algorithms (Park et al., 1999) to infer the shear-wave velocity profile beneath the acquisition location (in principle, phase velocities depend also on the compressional velocity and density, but, in the vast majority of the practical cases, that minor dependence is seldom exploited – see i.e. Xia et al., 1999).

Like many other inversion problems, also retrieving the shear-wave velocity profile is an ill-posed problem and the associated ambiguity is usually tackled by including a regularization term in the inversion process. Basically, the regularization term formalizes the prior information – different from the one provided by the collected data – about the physical system under investigation. In this way, through the proper choice of the regularization term, it is possible to select – among all the possible solutions compatible with the data – the unique and stable model that is also consistent with our expectations (described by the regularization). Thus, the regularization term plays a crucial role in the selection of the final result (in our specific case, the shear-wave velocity profile).

Despite its importance, usually, invocating a – perhaps,

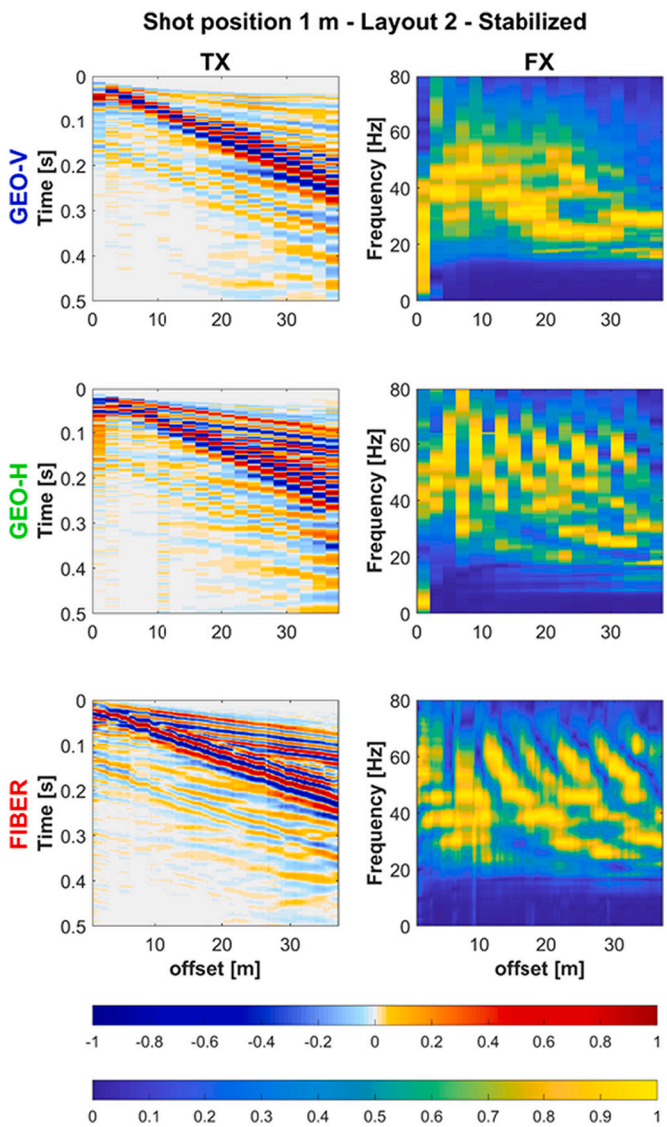

Fig. 8. Layout 2 (2 m geophone spacing) in the portion of stabilized ground. In the left column, the trace-normalized seismograms (TX) of (from top to bottom): vertical geophones (GEO-V), horizontal in-line geophones (GEO-H) and fiber optic sensors (FIBER). In the right column, the corresponding trace-normalized frequency content plotted as Fourier transforms of each trace (FX).

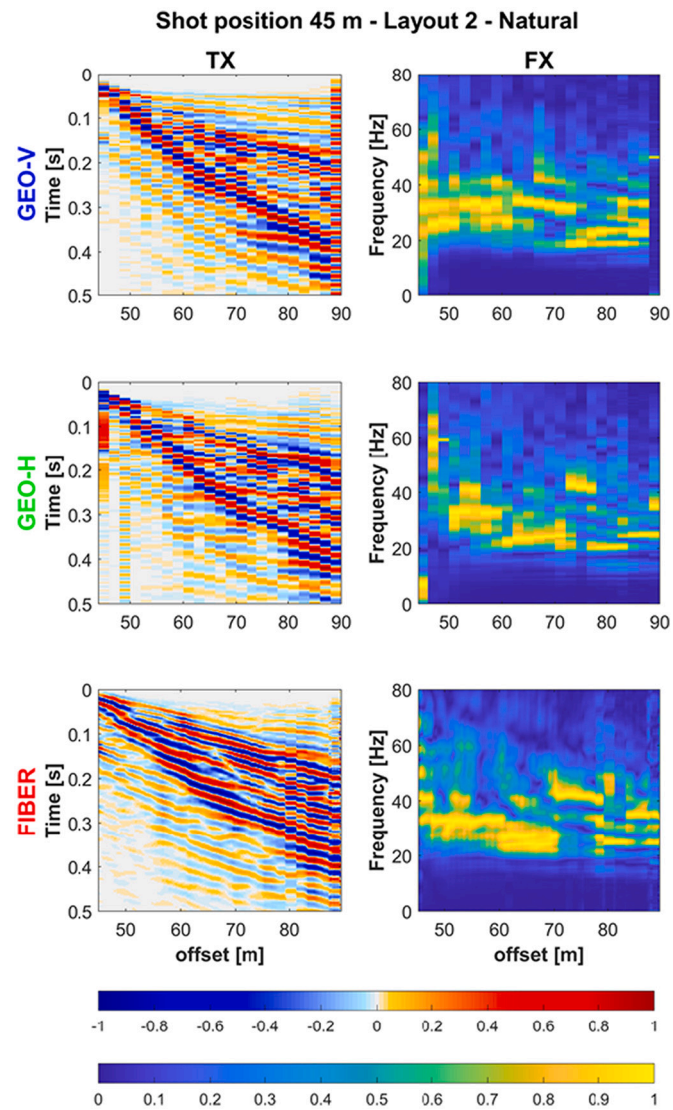

Fig. 9. Layout 2 (2 m geophone spacing) in the portion of natural ground. In the left column, the trace-normalized seismograms (TX) of (from top to bottom): vertical geophones (GEO-V), horizontal in-line geophones (GEO-H) and fiber optic sensors (FIBER). In the right column, the corresponding trace-normalized frequency content plotted as Fourier transforms of each trace (FX).

misinterpreted – Occam's Razor principle (Popper, 2005), the regularization term is chosen in order to favor smooth solutions (Zhdanov, 2002).

However, this choice can be often in contradiction with the actual nature of the subsurface, in which, for example, the presence of sharp boundaries can be possibly well-known; in these cases, the use of smooth regularizations would lead to incorrect results (even if perfectly compatible with the measurements).

In the present research, since we knew that, by construction, the subsurface consists of blocky targets and abrupt changes in the physical properties, we coherently adopt a tunable regularization term based on the minimum gradient support stabilizer (Zhdanov et al., 2006; Vignoli et al., 2015). The main characteristic of the adopted stabilizer lies in the capability of providing solutions (equally compatible with the measurements) with a tunable level of sparsity (Vignoli et al., 2021). The adopted tunable stabilizer, $s(\boldsymbol{\beta})$, has the following expression:

$$s(\boldsymbol{\beta}) = (\mathbf{L}\,\Delta\boldsymbol{\beta})^2 \Big/ \left((\mathbf{L}\,\Delta\boldsymbol{\beta})^2 + \varepsilon^2\right)^{-1/2} \tag{1}$$

where: $\mathbf{L}$ is a discrete approximation of the spatial derivative, $\Delta\boldsymbol{\beta} = (\boldsymbol{\beta} - \boldsymbol{\beta}_0)$ is the difference between the shear-wave velocity $\boldsymbol{\beta}$ and the reference model $\boldsymbol{\beta}_0$, while ε is the parameter used to tune the desired sparsity level of the solution and that should be selected accordingly to the scale and the characteristics of the target features to be reconstructed (Vignoli et al., 2021). In particular, the value of the tuning parameter ε is connected to the minimum velocity variation to be considered significant for the studied problem.

In the present examples, the subsoil has been parameterized with 1000 layers with a fixed thickness of 0.05 m; this is to avoid any possible effect of the parameterization on the final result and to make the regularization term act as the unique inversion stabilizer. Hence, by following the prescriptions in Vignoli et al. (2021), the tuning parameter has been chosen equal to $\varepsilon = 0.6$ (for all the inverted datasets); this specific value, together with the used discretization, promotes the retrieval of velocity models characterized by (sharp) changes larger than a few tens of meters per seconds over a 1 m depth interval.

Concerning the choice for the reference model, $\boldsymbol{\beta}_0$, it has been selected homogeneous and, so, characterized by a unique velocity equal

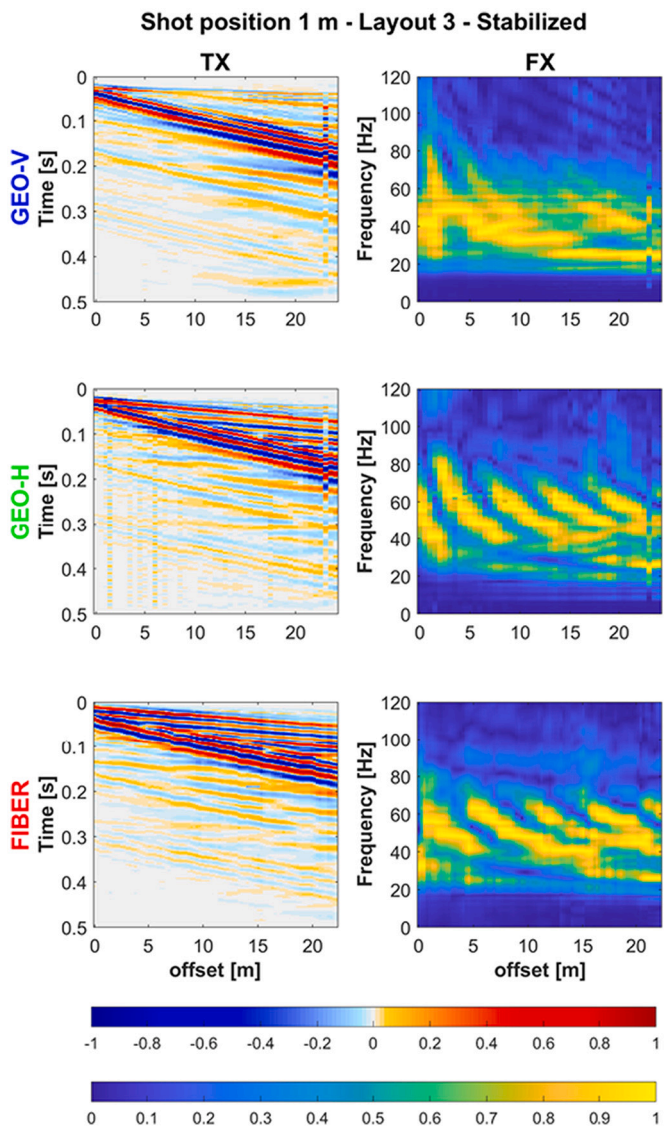

Fig. 10. Layout 3 (0.5 m geophone spacing) in the portion of stabilized ground. In the left column, the trace-normalized seismograms (TX) of (from top to bottom): vertical geophones (GEO-V), horizontal in-line geophones (GEO-H) and fiber optic sensors (FIBER). In the right column, the corresponding trace-normalized frequency content plotted as Fourier transforms of each trace (FX).

to 400 m/s. This specific value for the reference model (that, for consistency, is also the starting model) could be easily inferred by the dispersion curves at low frequencies. In any case, it can be easily shown (Vignoli et al., 2021; Vignoli et al., 2012) that this regularization strategy is quite robust with respect to different choices of the starting/reference model (obviously above the Depth Of Investigation (DOI), i.e., the depth where the sensitivity of the data to the inversion model parameters drops significantly).

In the original work by Vignoli et al. (2021), it is demonstrated how different values of the tuning parameters can be used to explore the model space and how the best value range is generally chosen based on the scale of the application (from crustal studies to near-surface investigations). However, the goal of the present research is to assess the performances of DAS data with respect to the standard geophones for geotechnical characterizations (in particular, in presence of artificial soil stabilization). Thus, an in-depth study of the impacts of the tuning parameters choices would be out of the scope of the present paper; for that, we invite the readers to refer to Vignoli et al. (2021), and, possibly, also to its recent extension to the two-dimensional case discussed in Guillemoteau et al. (2022).

3. Results and discussion

DAS data are always acquired along the entire length of the buried fiber optic cable, but, for sake of comparison, we selected the samples across the same transect as for the geophone layout for every single shot.

Fig. 5 illustrates an example of seismograms, unfiltered and trace-normalized, for the Layout 1 configuration. DAS data has a higher spatial and temporal resolution (see Table 1).

The seismograms show high similarity, and the same seismic events can be recognized. In all the three acquisitions, it is particularly visible the transition zone between the topographically higher stabilized ground (from 0 to 38 m) and the natural ground (from 42 to 88 m). It is evident that the seismogram of the DAS acquisition (FIBER) is more similar to the horizontal in-line component of the geophones (GEO-H). DAS does not discriminate between the different spatial components of the ground movements and its sensitivity is a function of the angle of incidence of acoustic waves (Wu et al., 2017): the fiber optic is more sensitive to compressional (P) waves with low-degrees of incident angle (waves propagating in the same direction of the cable), whereas it is essentially blind to events that propagate perpendicular to the fiber optics. The strongest DAS response to shear (S) waves occurs when the incident angle is around 45 degrees and damps down to no recorded signal for higher and lower incident angles.

Despite a general likeness between fiber optics and geophones acquisitions, a relevant aspect to be mentioned is the combined effect of spatial resolution (Gauge length) and spatial sampling of DAS surveys. We acquired a seismic trace every 0.255 m along the fiber with a Gauge length of 2 m (Table 1). The outcome of these parameters is a localized "stepwise" appearance of the seismic events in the DAS data, as it is particularly evident in Fig. 6, which shows the seismograms of Layout 3. The horizontal geophones (left plot) have a punctual resolution and a spatial sampling of 0.5 m. Even if the spatial frequency is lower than for the fiber optic data, the seismogram looks smoother, and the seismic events have a more linear appearance. Instead, the DAS seismogram (right plot in Fig. 6) shows a "stepwise" behavior that is more pronounced in some portions of the profile, reaching a maximum of 6 adjacent traces (between 8 and 9 m) displaying a similar pattern, especially at traveltimes around 0.1 s. The same pattern is present in all the acquisitions independently from the location of the source.

The integration along the Gauge length acts as a moving average window (Dean et al., 2017). Along the 2 m resolution segment, some points can record a stronger signal that is dominant and commonly present in a few traces. The stronger signal at some points can be caused by a local more effective coupling of the cable with the surrounding material. This localized and more intense stretching of the optic fiber may mask the weaker signals from the other portions of the 2 m segment (Gauge length). The cable construction (e.g., the distribution of scattering points along the glass fiber) can also play a role in defining how the fiber optic responds to external vibrations, enhancing the signal from specific portions of the Gauge length.

The acquired seismic data have been analyzed for the seismic refraction method (Fig. 7). A clear refracted event is recognizable in the vertical geophones (GEO-*V*) dataset, whereas it is very weak in the seismogram collected by horizontal in-line geophones (GEO-H), such that it is hardly detectable within 30 m from the source. The seismogram from the DAS acquisition does not show any refracted event, not even characterized by a weak signal. In Fig. 7, the picked refracted event from the GEO-V seismogram (blue dashed line) is superimposed on the other two datasets. From the bottom panel in Fig. 7, it is evident that no significant signal is present at those time-locations in the fiber optic data, and that DAS is recording merely high-frequency noise. This is consistent with the fact that refracted waves have a high angle of incidence at the surface, due to the slower shallower layer. As analyzed by Wu et al. (2017), DAS is mainly sensitive to P-waves propagating along the same

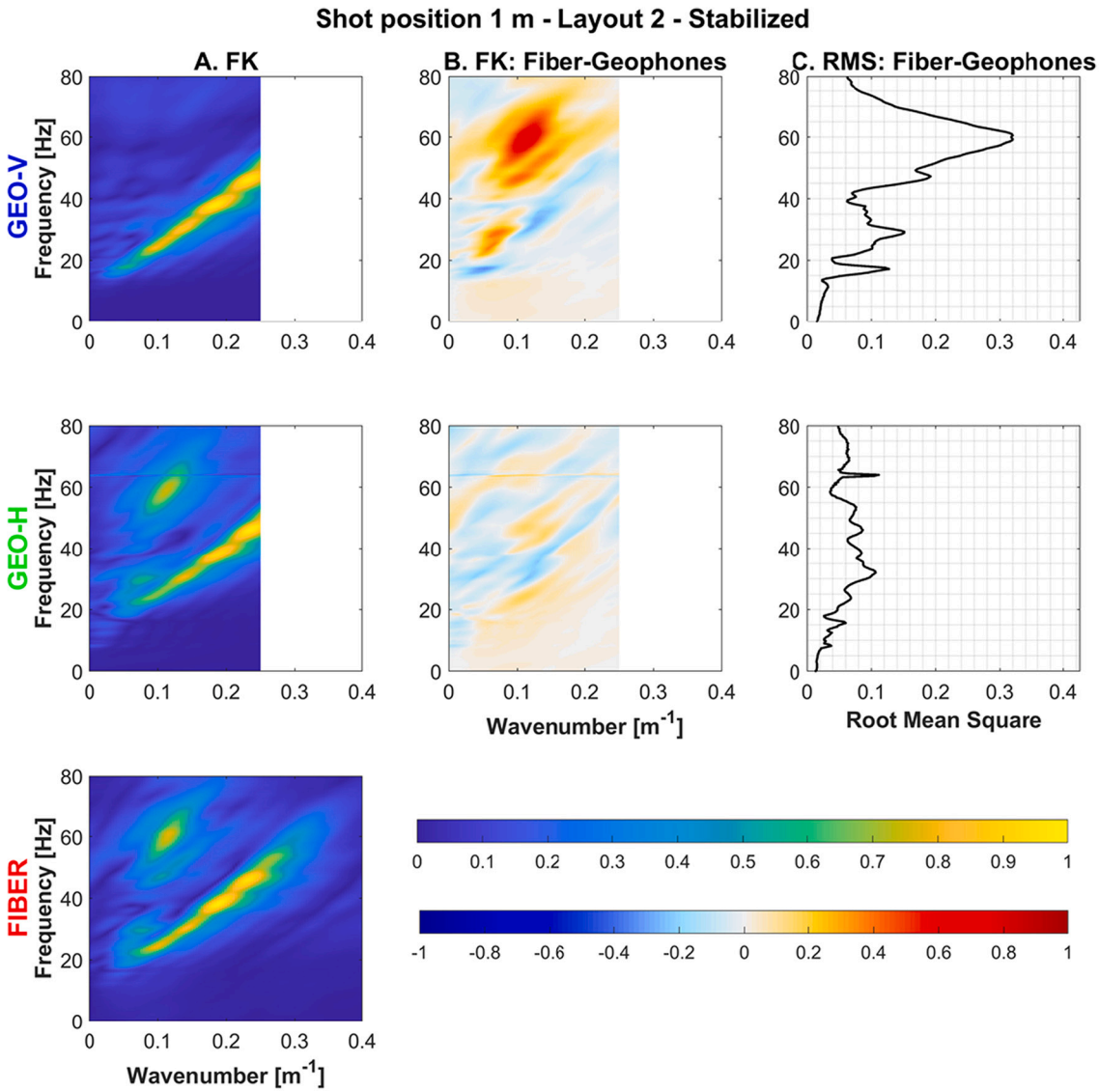

Fig. 11. Layout 2 (2 m geophone spacing) in the portion of stabilized ground. A, left column, the normalized spectra (FK) of (from top to bottom): vertical geophones (GEO-V), horizontal in-line geophones (GEO-H) and fiber optic sensors (FIBER). B, central column, the absolute difference between the normalized spectra of DAS and geophones. C, right column, RMS error of the same spectra for each frequency.

direction of the cable; consistently, for higher incident angles, the signal progressively fades, resulting in an unobservable refraction event.

Figs. 8 and 9 show the seismograms (left column) of Layout 2 for the geophones and fiber optics acquisitions; the profile has been subdivided into the portions associated with the stabilized and natural ground, respectively. Not surprisingly (improving the geotechnical characteristics is the ultimate goal of ground stabilization), the portion of untreated ground is characterized by slower velocities of the seismic events. The same figures display the spectral content of each trace (FX), in the right column. Also in this case, it is evident, especially considering the FX spectra, that the signal recorded by the DAS system shows a higher similarity with the horizontal geophones in both ground conditions.

The DAS seismogram of the natural ground (Fig. 9) reveals less pronounced "stepwise" features (see Fig. 6) compared to the portion of stabilized ground (Fig. 8), despite the identical fiber installation. This can be due to the different spectral content of the natural ground, characterized by lower frequencies, which are less affected by the Gauge length. Fig. 10 displays, for Layout 3, the same high similarity between the fiber optics and the horizontal geophones – in this specific case, characterized, by a higher spatial sampling (0.5 m).

With the aim of thoroughly analyzing the spectral content of the recorded acoustic signal, a two-dimensional Fourier transform (FK) has been applied to the seismograms (Figs. 11–13). The similarity between the acoustic sensors is here quantified by analyzing the discrepancies of the energy distribution in the FK spectra normalized, frequency-by-frequency, for the corresponding amplitude maximum (columns B and C).

The most energetic dispersive event – related to surface waves propagation – is essentially identical for geophones and DAS receivers (columns B in Figs. 11 and 12), for which the larger spatial sampling of the geophones (2 m) results in a narrower wavenumber range. The most evident differences are between fiber optic sensors and vertical geophones, and they are related to seismic events with high frequencies and to higher modes of propagation of the surface waves. This is particularly clear by studying the frequency-by-frequency Root Mean Square (RMS) error (columns C in Figs. 11 and 12).

The higher lateral sampling rate of Layout 3 of the geophones acquisition allows analyzing shorter wavelengths (Fig. 13A). Despite the higher spatial sampling rate of the DAS data – almost twice the geophone's one – the DAS recorded signal shows a spectrum limited to

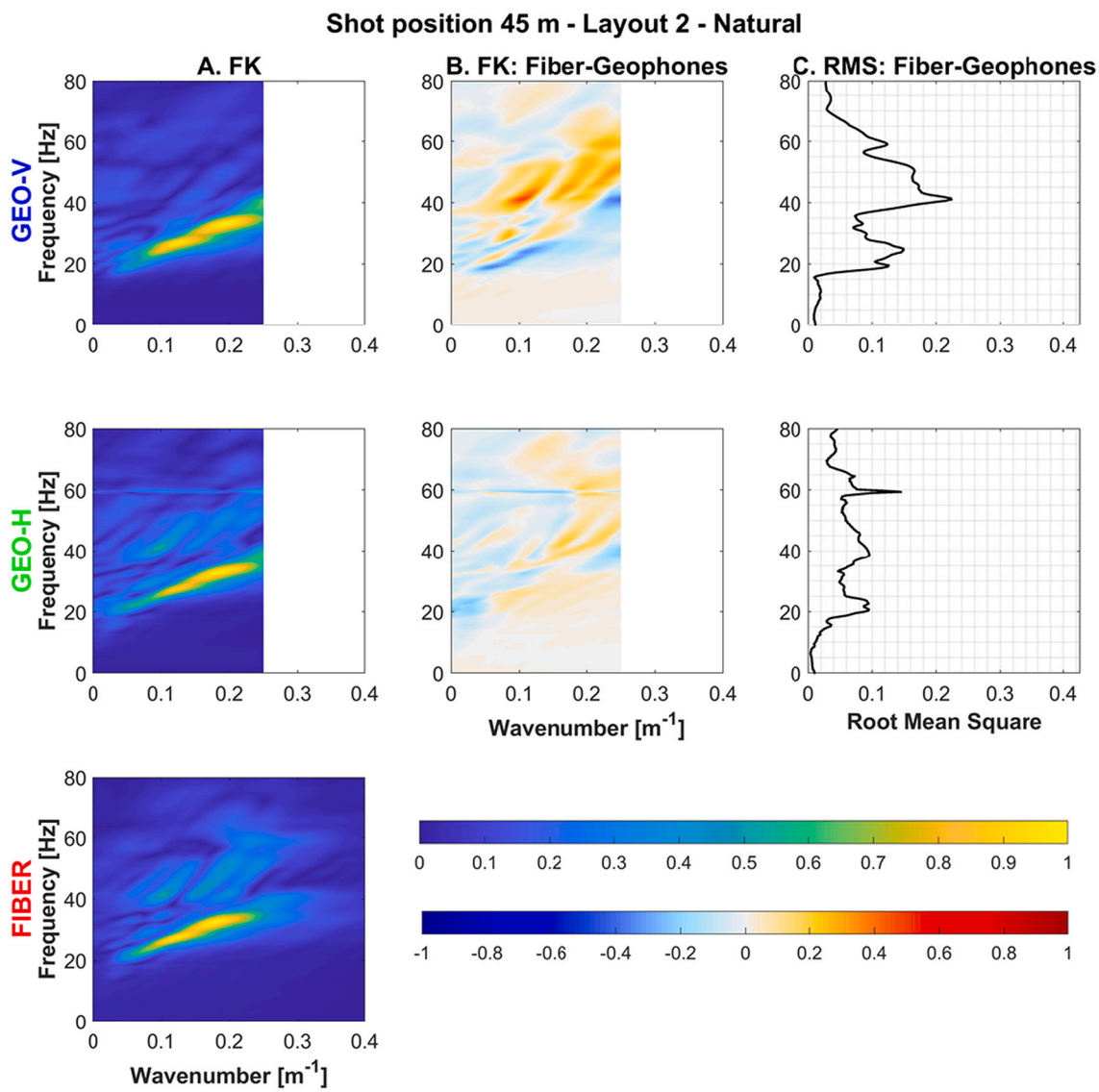

Fig. 12. Layout 2 (2 m geophone spacing) in the portion of natural ground. A, left column, the normalized spectra (FK) of (from top to bottom): vertical geophones (GEO-V), horizontal in-line geophones (GEO-H) and fiber optic sensors (FIBER). B, central column, the absolute difference between the normalized spectra of DAS and geophones. C, right column, RMS error of the same spectra for each frequency.

lower wavenumber values (Fig. 13B). The energy maxima of the lower mode of propagation of surface waves (possibly the fundamental mode) are concentrated in the area of the FK spectrum with upper limits of 0.3–0.4 m^{-1} and around 60 Hz. This means that DAS does not sense wavelengths shorter than about 1.25–1.5 m, even if, theoretically, the spatial sampling allows the system to record wavelengths larger than 0.51 m. The shorter wavelengths could not be represented due to the resolution driven by the 2 m Gauge length, which acts as a low-pass filter.

The maximum amplitude of the FK spectra has been picked at each frequency for the three different recording settings (vertical and horizontal geophones, and DAS). The picking results are plotted together for sake of comparison in Fig. 14. The slower and most energetic mode of propagation of surface waves (from here below assumed to be – and correspondingly named – "fundamental mode") coincides between the different receiver settings, whereas the higher modes of propagation (characterized by higher frequencies and lower amplitude) are only partially consistent. The different records obtained with the different sensors have comparable modes of propagation within a small variance due to inevitable environmental noise. The higher resolution of the geophones in Layout 3 (Fig. 14C) allows identifying the fundamental mode of surface waves propagation across a larger range. If DAS is compared with geophones of Layouts 1 and 2 (Fig. 14A and B), the fundamental modes are essentially superimposed. Only for the faster stabilized ground (Fig. 14A), the fiber optics (red dots) are capable to record higher frequencies for the fundamental mode: almost 60 Hz compared to approximately 50 Hz of the spectra extracted from the geophones data.

The goal of ground stabilization procedures is to enhance the mechanical properties of the original natural sediments. The shear modulus is a relevant parameter for the geotechnical characterization of the ground related to infrastructure building and depends on the shear wave velocities (Vs). For this reason, the fundamental mode of Rayleigh waves has been extracted and inverted to obtain a vertical one-dimensional profile of Vs (Fig. 15).

Fig. 15A shows the results of the inversion of the dispersion curve data extracted from some of the maxima of the FK spectra in Fig. 14 (associated with different portions of stabilized and natural ground). The Vs profiles derived by the acquisition on the natural ground (dashed lines in Fig. 15A) are vertically shifted by 0.75 m to compensate for the

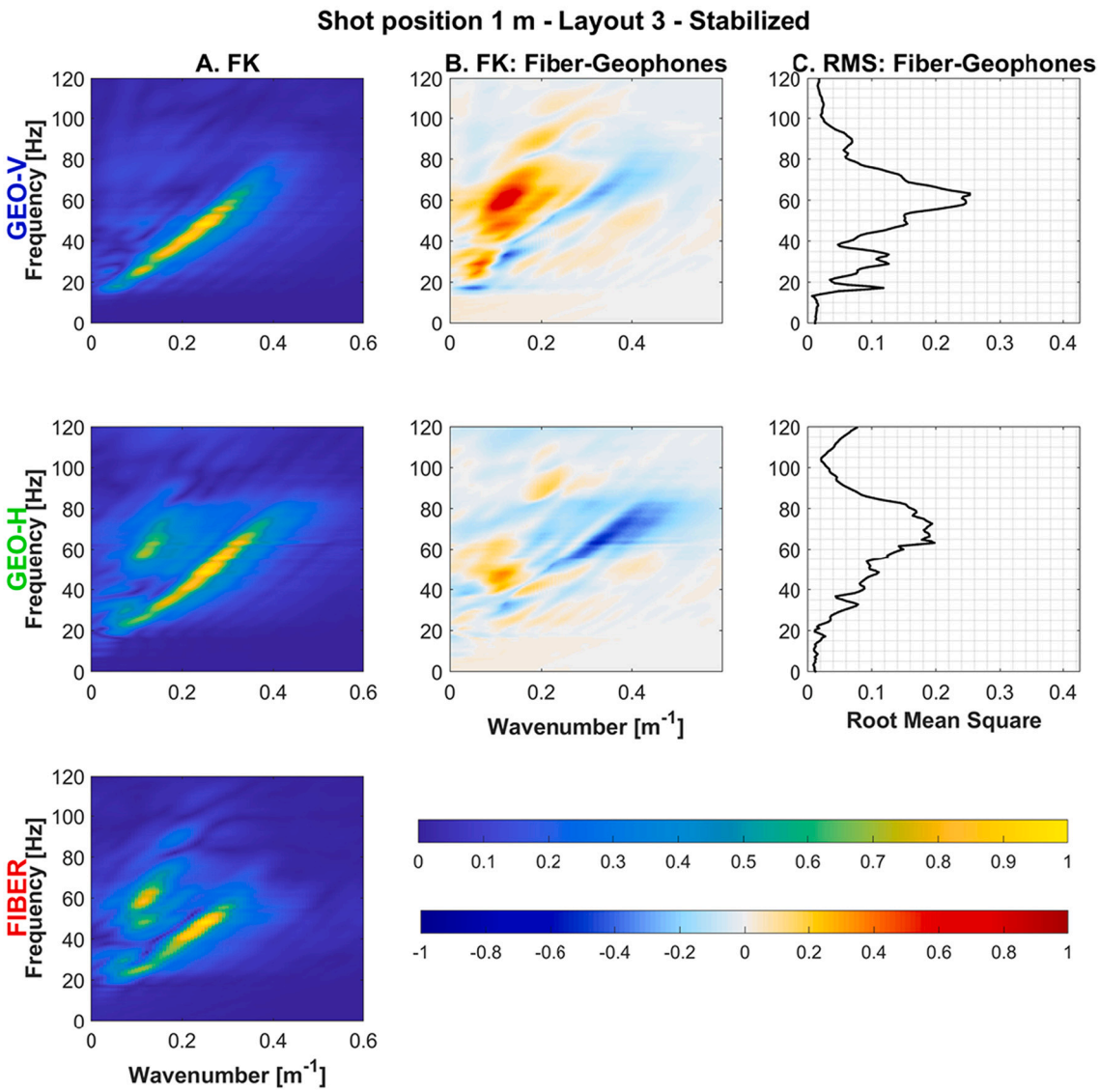

Fig. 13. Layout 3 (0.5 m geophone spacing) in the portion of stabilized ground. A, left column, the normalized spectra (FK) of (from top to bottom): vertical geophones (GEO-V), horizontal in-line geophones (GEO-H) and fiber optic sensors (FIBER). B, central column, the absolute difference between the normalized spectra of DAS and geophones. C, right column, RMS error of the same spectra for each frequency.

mean elevation difference with respect to the artificial ground (Fig. 4B). Fig. 15B displays the experimental and the calculated dispersion curves of the fundamental mode for each inverted layout: i) the gray error-bars show the phase-velocities (V_R) extracted by the data, together with the associated uncertainty (estimated via several repetitions with the same source location); whereas the colored lines are the V_R curves calculated from the unidimensional Vs distribution inferred via the inversion.

From Fig. 15A, it clearly appears as the reconstructed Vs distributions are consistent between the different acquisition techniques, especially, at shallow, where a low-velocity layer (Vs < 250 m/s) is identified between 0 and 3 m below the topographic surface. The almost perfect matching between the inversion results, associated:

i) on one hand, for the stabilized portion, with the two different geophone Layouts (Layout 3 and the combined Layout 1 + 2); and
ii) on the other hand, for the natural ground, with the DAS and the combined geophones Layout 1 + 2 data,

are particularly impressive and demonstrate the extreme reliability of the surface wave for the reconstruction of even relatively complex shear-modulus profiles. The only significant mismatch occurs, at depth (> 4 m) for the stabilized ground and between the fiber (solid red line) and the geophone (solid blue and cyan lines) results; this discrepancy is caused by the higher phase velocities recorded by the DAS at a lower frequency. The higher velocity recorded by the DAS in the low-frequency range (< 25 Hz) is visible comparing the 1st, 2nd, and the 4th panels in Fig. 15B (blue, cyan, and red solid lines). This higher phase velocity recorded by the fibers is a consequence of the broader amplitude peak of the FK spectrum in that frequency range with respect to the corresponding vertical geophone (in this respect, compare the top and bottom panels of Fig. 13A). This is consistent with the fact that the measurements recorded by the fiber optics are a combination (i.e., a weighted average) of the vertical and horizontal components of the signal propagating from the source (e.g., Kennett, 2022).

Considering again Fig. 15A, and – in particular, comparing the solid (corresponding to the measurements over the stabilized ground) and the dashed (associated with the natural ground) lines – within the shallowest 4 m, it is not surprising that the ground stabilization procedure increased the Vs values by approximately 50–100 m/s (hence by around 60% of the original velocity) with respect to the natural ground. More

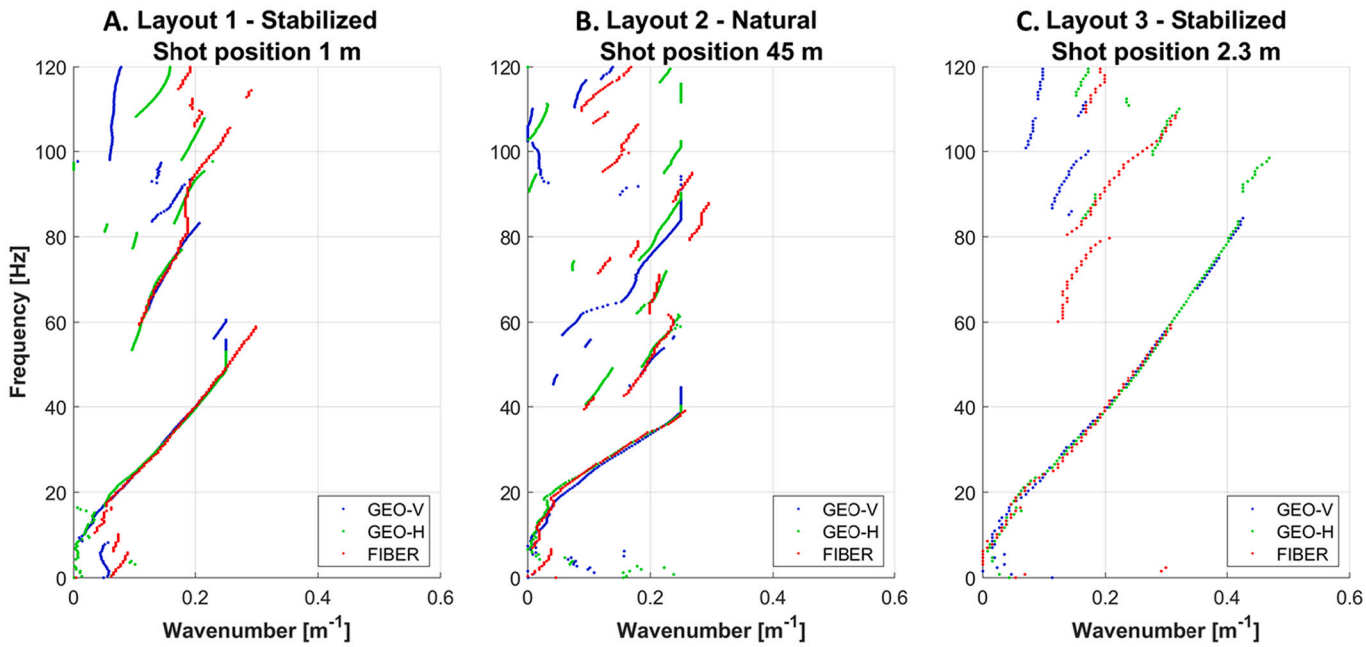

Fig. 14. Comparison of the modes of propagation among vertical geophones (blue dots), horizontal in-line geophones (green dots) and fiber optic sensors (red dots). Data are extracted from: A. Layout 1 on stabilized ground, B. Layout 2 on natural ground, C. Layout 3 on Stabilized ground. The points defining the propagation modes consist of the maxima picked, frequency-by-frequency, on the FK spectra. (For interpretation of the references to colour in this figure legend, the reader is referred to the web version of this article.)

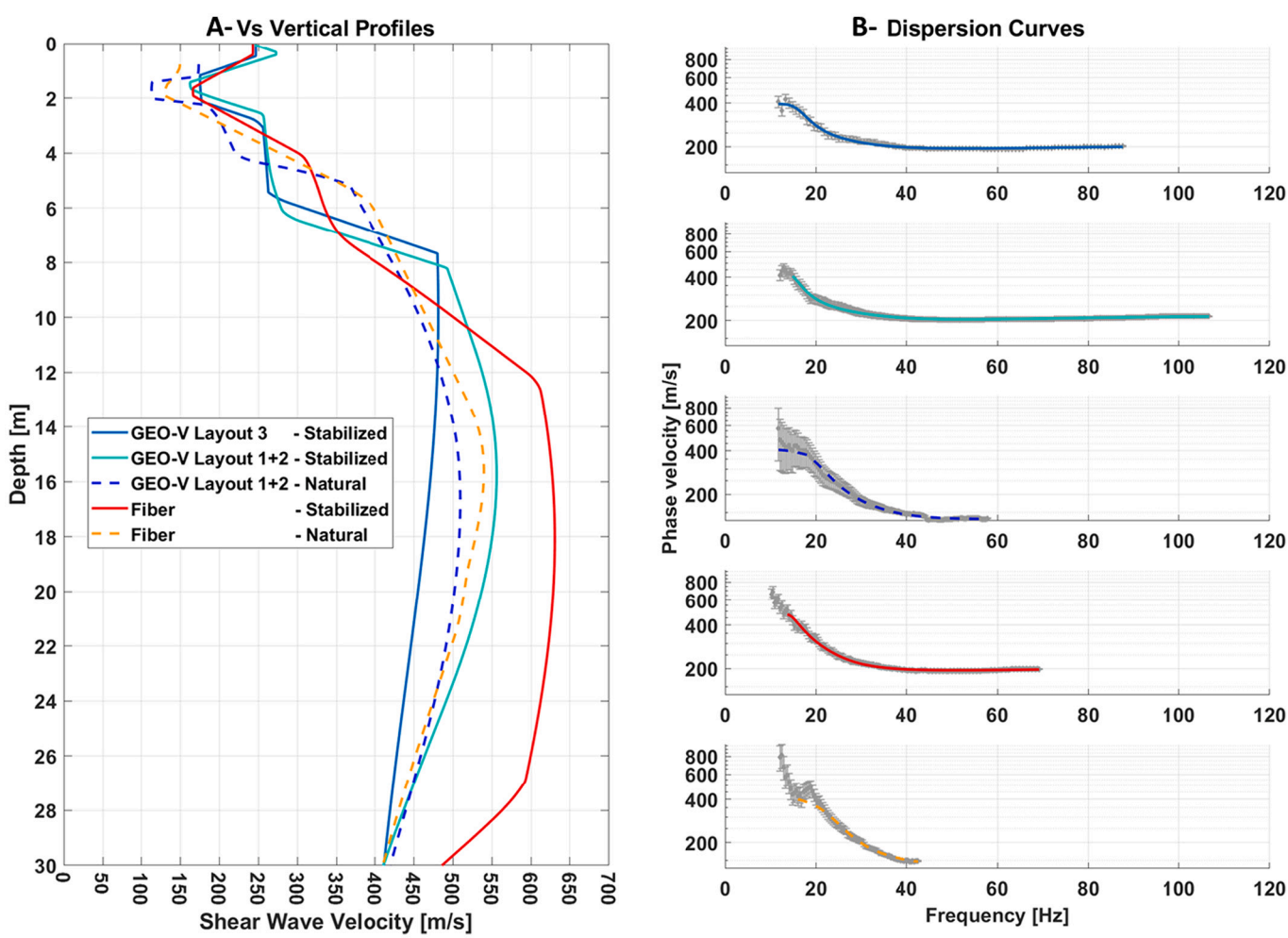

Fig. 15. Vertical profiles of inverted shear-wave velocities (A) from the dispersion curves of surface waves (B). In B, the data plotted in gray are the experimental dispersion curves of the fundamental mode; the relative error bars represent the standard deviation. The colored lines are the calculated dispersion curves (same legend as A).

specifically, a clear effect of the stabilization is evident in the shallower 2 m, whereas, from 2 to 4 m, the increased velocity is a consequence of the repeated mechanical compaction operated during the construction of the artificial ground.

The bedrock shows Vs values larger than 400 m/s and it can be identified at a depth of around 8 m. The differences between the inferred depths for the natural and stabilized ground are compatible with the typical spatial variability of the geology in the area, especially if we consider a weathered rock layer of 1.5 m thickness, as confirmed by nearby drilling.

4. Conclusions

The present work is a feasibility study on the application of fiber optics as acoustic sensors for civil engineering investigations in connection with ground stabilization, focusing on the comparison with standard acoustic sensors (geophones).

The results clearly show that the signal from the fiber optics, despite the inevitable differences with respect to the different components collected via the standard geophones, can be a valid alternative to standard seismic receivers for specific applications. As a general conclusion, DAS is a methodology that can prove to be a powerful tool for near-surface geophysical studies in environmental and civil engineering applications.

The signal from the DAS system is almost equivalent to standard seismic receivers. As it was expected, fiber optics display a higher similarity with the horizontal in-line component of the geophones, as they record the longitudinal stretching of the fiber. On the other hand, DAS is less sensitive to acoustic waves propagating perpendicularly to fiber cable. For this reason, a refracted event was not detectable via DAS despite the good coupling between the fiber optics cable and the ground. In turn, this highlights that DAS might not be the best tool for geotechnical characterization via refraction seismics.

The frequency content of the DAS system is strongly related to the resolution of the technique, which depends on the Gauge length (2 m in the present work). Such resolution makes DAS less sensitive to smaller wavelengths compared to short-spacing geophones. It must be mentioned that seismic surveys are rarely conducted with an intra-geophone spacing of less than 1 m. The uncertainty of the relative location of the receivers, especially on a rugged topographic surface, usually makes traditional seismic measurements impractical with a spatial resolution smaller than 0.5 m. On the other hand, the exact location of the receiver position along the fiber optics is a great advantage of the DAS acquisitions.

The vertical profiles of inverted shear-wave velocities from the DAS dataset are comparable with the same profiles obtained from traditional acquisitions through geophones. A similar improvement of the mechanical properties is identified with both technologies, even if the shear-wave velocities increase by about 50–100 m/s in the area of the stabilized ground.

The specifications of the DAS instrument applied in the project (spatial resolution of 2 m and spatial sampling interval of 0.255 m) are probably the minimum requirements for these types of engineering applications. Considering that DAS is a recent technological development, this limit might be overtaken in the future, paving the way for broader ranges of applications.

Thus, briefly, the novelties of the discussed approach and tests concern:

i) The effectiveness of geophysical methods (and, in particular, surface wave inversion) for the reconstruction of geotechnical parameters (when properly used; for example, with the use of the proper regularization);
ii) The unavoidable differences between standard geophones and the new fiber sensors in terms of recorded seismic responses;
iii) The fact that, despite the differences with respect to the geophones, DAS data can be considered, for specific applications, a valid alternative to more traditional techniques.

Declaration of Competing Interest

The authors declare that they have no known competing financial interests or personal relationships that could have appeared to influence the work reported in this paper.

Acknowledgements

The authors would acknowledge *V*innova, InfraSweden 2030 (2018-00641 – Kvalitetskontroll av. markstabilisering genom seismisk mätning med optisk Fiber), SBUF (Svenska Byggbranschens Utvecklingsfond; ID: 13579) and BeFo (Stiftelsen Bergteknisk Forsking) for the financial support. The partners of the project Hydroresearch AB and Silixa ltd have been supporting and showing flexibility modifying the plans of the project. A special thanks to Impakt Geofysik AB for the help in the field survey. A particular acknowledgement goes to Skanska Sverige AB for the availability and the great support on the ESS construction site, especially for the help with the installation of the fiber optics cable and for sharing nearby geotechnical data. Finally, thanks to the European Spallation Source, ESS, for allowing us on the site for this experiment.

References

Alfataierge, E., Aldawood, A., Bakulin, A., Stewart, R.R., Merry, H., 2020. Influence of gauge length on DAS VSP data at the Houston Research Center Test Well. In: SEG Technical Program Expanded Abstracts 2020. Society of Exploration Geophysicists, pp. 505–509.

Bergamo, P., Boiero, D., Socco, L.V., 2012. Retrieving 2D structures from surface-wave data by means of space-varying spatial windowing. Geophysics 77 (4), EN39–EN51.

Binder, G., Titov, A., Liu, Y., Simmons, J., Tura, A., Byerley, G., Monk, D., 2020. Modeling the seismic response of individual hydraulic fracturing stages observed in a time-lapse distributed acoustic sensing vertical seismic profiling survey. Geophysics 85, T225–T235. https://doi.org/10.1190/geo2019-0819.1.

Cheng, F., Chi, B., Lindsey, N.J., Dawe, T.C., Ajo-Franklin, J.B., 2021. Utilizing distributed acoustic sensing and ocean bottom fiber optic cables for submarine structural characterization. Sci. Rep. 11, 1–14. https://doi.org/10.1038/s41598-021-84845-y.

Coni, M., Portas, S., Maltinti, F., Pinna, F., 2018. Sealing of paving stone joints. Int. J. Pavement Res. Technol. 11 (8), 813–818.

Coni, M., Mistretta, F., Stochino, F., Rombi, J., Sassu, M., Puppio, M.L., 2021. Fast falling weight deflectometer method for condition assessment of RC bridges. Appl. Sci. 11 (4), 1743.

Dean, T., Cuny, T., Hartog, A.H., 2017. The effect of gauge length on axially incident P-waves measured using fibre optic distributed vibration sensing. Geophys. Prospect. 65, 184–193. https://doi.org/10.1111/1365-2478.12419.

Donohue, S., Long, M., 2008. Ground improvement assessment of glacial till using shear wave velocity. In: Geotech. Geophys. Site Charact. Proc. 3rd Int. Conf. Site Charact. ISC'3, pp. 825–830.

Dou, S., Lindsey, N., Wagner, A.M., Daley, T.M., Freifeld, B., Robertson, M., Peterson, J., Ulrich, C., Martin, E.R., Ajo-Franklin, J.B., 2017. Distributed acoustic sensing for seismic monitoring of the near surface: a traffic-noise interferometry case study. Sci. Rep. 7, 1–12. https://doi.org/10.1038/s41598-017-11986-4.

Fernández-Ruiz, M.R., Soto, M.A., Williams, E.F., Martin-Lopez, S., Zhan, Z., Gonzalez-Herraez, M., Martins, H.F., 2020. Distributed acoustic sensing for seismic activity monitoring. APL Photon. 5 https://doi.org/10.1063/1.5139602.

Firoozi, Ali Akbar, Guney Olgun, C., Firoozi, Ali Asghar, Baghini, M.S., 2017. Fundamentals of soil stabilization. Int. J. Geo-Eng. 8 https://doi.org/10.1186/s40703-017-0064-9.

Guillemoteau, J., Vignoli, G., Barreto, J., Sauvin, G., 2022. Sparse laterally constrained inversion of surface wave dispersion curves via minimum gradient support regularization. Geophysics 87 (3), 1–38.

Hartog, A.H., 2017. An Introduction to Distributed Optical Fibre Sensors. CRC Press.

Kara De Maeijer, P., Luyckx, G., Vuye, C., Voet, E., Vanlanduit, S., Braspenninckx, J., Stevens, N., De Wolf, J., 2019. Fiber optics sensors in asphalt pavement: state-of-the-art review. Infrastructures 4 (2), 36.

Kennett, B.L., 2022. The seismic wavefield as seen by distributed acoustic sensing arrays: local, regional and teleseismic sources. Proc. R. Soc. A 478 (2258), 20210812.

Lai, C.G., Rix, G.J., Foti, S., Roma, V., 2002. Simultaneous measurement and inversion of surface wave dispersion and attenuation curves. Soil Dyn. Earthq. Eng. 22 (9–12), 923–930.

Lin, C.H., Lin, C.P., Dai, Y.Z., Chien, C.J., 2017. Application of surface wave method in assessment of ground modification with improvement columns. J. Appl. Geophys. 142, 14–22. https://doi.org/10.1016/j.jappgeo.2017.05.007.

Lindsey, N.J., Rademacher, H., Ajo-Franklin, J.B., 2020. On the broadband instrument response of fiber-optic DAS arrays. J. Geophys. Res. Solid Earth 125, 1–16. https://doi.org/10.1029/2019JB018145.

Lior, I., Sladen, A., Rivet, D., Ampuero, J.P., Hello, Y., Becerril, C., Martins, H.F., Lamare, P., Jestin, C., Tsagkli, S., Markou, C., 2021. On the detection capabilities of underwater distributed acoustic sensing. J. Geophys. Res. Solid Earth 126, 1–20. https://doi.org/10.1029/2020JB020925.

Luo, B., Lellouch, A., Jin, G., Biondi, B., Simmons, J., 2021a. Seismic inversion of shale reservoir properties using microseismic-induced guided waves recorded by distributed acoustic sensing. Geophysics 86, R383–R397. https://doi.org/10.1190/geo2020-0607.1.

Luo, B., Trainor-Guitton, W., Bozdag, E., LaFlame, L., Cole, S., Karrenbach, M., 2021b. Horizontally orthogonal distributed acoustic sensing array for earthquake- and ambient-noise-based multichannel analysis of surface waves. Geophys. J. Int. 222, 2147–2161. https://doi.org/10.1093/GJI/GGAA293.

Miskiewicz, M., Lachowicz, J., Tysiac, P., Jaskula, P., Wilde, K., 2018. The application of non-destructive methods in the diagnostics of the approach pavement at the bridges. IOP Conf. Ser. Mater. Sci. Eng. 356 (1), 012023.

Nishimura, T., Emoto, K., Nakahara, H., Miura, S., Yamamoto, M., Sugimura, S., Ishikawa, A., Kimura, T., 2021. Source location of volcanic earthquakes and subsurface characterization using fiber-optic cable and distributed acoustic sensing system. Sci. Rep. 11, 1–12. https://doi.org/10.1038/s41598-021-85621-8.

Park, C.B., Miller, R.D., Xia, J., 1999. Multichannel analysis of surface waves. Geophysics 64 (3), 800–808.

Popper, K., 2005. The Logic of Scientific Discovery. Routledge.

Socco, L.V., Foti, S., Boiero, D., 2010. Surface-wave analysis for building near-surface velocity models—established approaches and new perspectives. Geophysics 75 (5), 75A83–75A102.

Soga, K., Luo, L., 2018. Distributed fiber optics sensors for civil engineering infrastructure sensing. J. Struct. Integr. Maint. 3, 1–21. https://doi.org/10.1080/24705314.2018.1426138.

Titov, A., Binder, G., Liu, Y., Jin, G., Simmons, J., Tura, A., Monk, D., Byerley, G., Yates, M., 2021. Modeling and interpretation of scattered waves in interstage distributed acoustic sensing vertical seismic profiling survey. Geophysics 86, D93–D102. https://doi.org/10.1190/geo2020-0293.1.

Vignoli, G., Strobbia, C., Cassiani, G., Vermeer, P., 2011. Statistical multioffset phase analysis for surface-wave processing in laterally varying media. Geophysics 76 (2), U1–U11.

Vignoli, Giulio, Deiana, Rita, Cassiani, Giorgio, 2012. Focused inversion of vertical radar profile (VRP) traveltime data. Geophysics 77 (1), H9–H18. https://doi.org/10.1190/geo2011-0147.1.

Vignoli, G., Fiandaca, G., Christiansen, A.V., Kirkegaard, C., Auken, E., 2015. Sharp spatially constrained inversion with applications to transient electromagnetic data. Geophys. Prospect. 63 (1), 243–255.

Vignoli, G., Gervasio, I., Brancatelli, G., Boaga, J., Della Vedova, B., Cassiani, G., 2016. Frequency-dependent multi-offset phase analysis of surface waves: an example of high-resolution characterization of a riparian aquifer. Geophys. Prospect. 64 (1), 102–111.

Vignoli, G., Guillemoteau, J., Barreto, J., Rossi, M., 2021. Reconstruction, with tunable sparsity levels, of shear wave velocity profiles from surface wave data. Geophys. J. Int. 225 (3), 1935–1951.

Walter, F., Gräff, D., Lindner, F., Paitz, P., Köpfli, M., Chmiel, M., Fichtner, A., 2020. Distributed acoustic sensing of microseismic sources and wave propagation in glaciated terrain. Nat. Commun. 11 https://doi.org/10.1038/s41467-020-15824-6.

Wang, H., Al-Qadi, I.L., Portas, S., Coni, M., 2013. Three-dimensional finite element modeling of instrumented airport runway pavement responses. Transp. Res. Rec. 2367 (1), 76–83.

Wilson, G.A., Willis, M.E., Ellmauthaler, A., 2021. Evaluating 3D and 4D DAS VSP image quality of subsea carbon storage. Lead. Edge 40, 261–266. https://doi.org/10.1190/tle40040261.1.

Wu, X., Willis, M.E., Palacios, W., Ellmauthaler, A., Barrios, O., Shaw, S., Quinn, D., 2017. Compressional-and shear-wave studies of distributed acoustic sensing acquired vertical seismic profile data. Lead. Edge 36, 987–993. https://doi.org/10.1190/tle36120987.1.

Xia, J., Miller, R.D., Park, C.B., Hunter, J.A., Harris, J.B., 1999. Evaluation of the MASW technique in unconsolidated sediments. In: SEG Technical Program Expanded Abstracts 1999. Society of Exploration Geophysicists, pp. 437–440.

Yuan, S., Lellouch, A., Clapp, R.G., Biondi, B., 2020. Near-surface characterization using a roadside distributed acoustic sensing array. Lead. Edge 39, 646–653. https://doi.org/10.1190/tle39090646.1.

Zhdanov, M.S., 2002. Geophysical Inverse Theory and Regularization Problems, vol. 36. Elsevier.

Zhdanov, M.S., Vignoli, G., Ueda, T., 2006. Sharp boundary inversion in crosswell travel-time tomography. J. Geophys. Eng. 3 (2), 122–134.